

---

*Research Article: New Research | Disorders of the Nervous System*

## **Dopamine development in the mouse orbital prefrontal cortex is protracted and sensitive to amphetamine in adolescence**

### **Adolescent dopamine development in the orbital PFC**

**Daniel Hoops<sup>a</sup>, Lauren M. Reynolds<sup>a,b</sup>, Jose-Maria Restrepo-Lozano<sup>a,b</sup> and Cecilia Flores<sup>a</sup>**

<sup>a</sup>*Department of Psychiatry, Douglas Mental Health University Institute, McGill University, 6875 LaSalle Boulevard, Montreal, Quebec H4H 1R3, Canada*

<sup>b</sup>*Integrated Program in Neuroscience, McGill University, 1033 Pine Avenue West, Montreal, Quebec H3A 1A1, Canada*

DOI: 10.1523/ENEURO.0372-17.2017

Received: 31 October 2017

Revised: 14 December 2017

Accepted: 15 December 2017

Published: 8 January 2018

---

**Author Contributions:** DH and CF conceived and designed the experiments. DH, LMR, and J-MRL conducted the experiments. DH and CF analyzed the data and drafted the manuscript.

**Funding:** <http://doi.org/10.13039/100000026HHS> | NIH | National Institute on Drug Abuse (NIDA)  
R01DA037911  
F31DA041188

**Funding:** National Science and Engineering Research Council of Canada (NSERC)  
2982226

**Funding:** <http://doi.org/10.13039/501100000024Gouvernement du Canada> | Canadian Institutes of Health Research (CIHR)  
MOP-74709

**Funding:** Quebec Nature and Technology Research Fund (FRQNT)  
208332

**Conflict of Interest:** Authors declare no conflict of interest.

This work was supported by the National Institute on Drug Abuse (R01DA037911 to CF; F31DA041188 to LMR), the Natural Science and Engineering Research Council of Canada (2982226 to CF), the Canadian Institutes of Health Research (MOP-74709 to CF) and the Quebec Nature and Technology Research Fund (208332 to DH). CF is a research scholar of the Fonds de Recherche du Québec - Santé.

**Correspondence should be addressed to** Dr. Cecilia Flores, Douglas Mental Health University Institute, (Perry Pavilion, room# 2111) 6875 LaSalle Blvd. Montréal (Verdun), QC H4H 1R3, Canada, Phone (514) 761-6131 ext: 2814; Fax: (514) 762-3034; Email: [cecilia.flores@mcgill.ca](mailto:cecilia.flores@mcgill.ca)

**Cite as:** eNeuro 2018; 10.1523/ENEURO.0372-17.2017

**Alerts:** Sign up at [eneuro.org/alerts](http://eneuro.org/alerts) to receive customized email alerts when the fully formatted version of this article is published.

Accepted manuscripts are peer-reviewed but have not been through the copyediting, formatting, or proofreading process.

Copyright © 2018 Hoops et al.

This is an open-access article distributed under the terms of the Creative Commons Attribution 4.0 International license, which permits unrestricted use, distribution and reproduction in any medium provided that the original work is properly attributed.

1 **Dopamine development in the mouse orbital prefrontal cortex is protracted and sensitive**  
2 **to amphetamine in adolescence**

3 **Abbreviated Title:** Adolescent dopamine development in the orbital PFC

4 Daniel Hoops<sup>a</sup>, Lauren M. Reynolds<sup>a,b</sup>, Jose-Maria Restrepo-Lozano<sup>a,b</sup>, & Cecilia Flores<sup>a\*</sup>

5 <sup>a</sup> Department of Psychiatry, Douglas Mental Health University Institute, McGill University,  
6 6875 LaSalle Boulevard, Montreal, Quebec, H4H 1R3, Canada

7 <sup>b</sup> Integrated Program in Neuroscience, McGill University, 1033 Pine Avenue West, Montréal,  
8 Québec, H3A 1A1, Canada

9 **Author Contributions:** DH and CF conceived and designed the experiments. DH, LMR, and J-  
10 MRL conducted the experiments. DH and CF analyzed the data and drafted the manuscript.

11 **\*Correspondence should be addressed to:**

12 Dr. Cecilia Flores

13 Douglas Mental Health University Institute

14 (Perry Pavilion, room# 2111) 6875 LaSalle Blvd. Montréal (Verdun), QC, Canada H4H 1R3

15 Phone (514) 761-6131 ext: 2814; Fax: (514) 762-3034; email: [cecilia.flores@mcgill.ca](mailto:cecilia.flores@mcgill.ca)

16 Number of Figures: 4; Number of Tables: 0; Number of Multimedia: 0

17 Number of words for Abstract: 243; Number of words for Significance Statement: 120

18 Number of words for Introduction: 584; Number of words for Discussion: 1609

19 **Conflict of Interest:** The authors declare no competing financial interests.

20 **Funding Sources:** This work was supported by the National Institute on Drug Abuse

21 (R01DA037911 to CF; F31DA041188 to LMR), the Natural Science and Engineering Research

22 Council of Canada (2982226 to CF), the Canadian Institutes of Health Research (MOP-74709

23 to CF) and the Quebec Nature and Technology Research Fund (208332 to DH). CF is a

24 research scholar of the Fonds de Recherche du Québec - Santé.

25 **Abstract**

26 The prefrontal cortex is divided into subregions including the medial and orbital prefrontal  
27 cortices. Dopamine connectivity in the medial prefrontal cortex continues to be established  
28 throughout adolescence as the result of the continuous growth of axons that innervated the  
29 nucleus accumbens prior to adolescence. During this period, dopamine axons remain  
30 vulnerable to environmental influences, such as drugs used recreationally by humans. The  
31 developmental trajectory of the orbital prefrontal dopamine innervation remains almost  
32 completely unstudied. Nonetheless, the orbital prefrontal cortex is critical for some of the  
33 most complex functions of the prefrontal cortex and is disrupted by drugs of abuse, both in  
34 adolescent humans and rodents. Here, we use quantitative neuroanatomy, axon-initiated  
35 viral-vector recombination, and pharmacology in mice to determine the spatiotemporal  
36 development of the dopamine innervation to the orbital prefrontal cortex and its  
37 vulnerability to amphetamine in adolescence. We find that dopamine innervation to the  
38 orbital prefrontal cortex also continues to increase during adolescence and that this  
39 increase is due to the growth of new dopamine axons to this region. Furthermore,  
40 amphetamine in adolescence dramatically reduces the number of presynaptic sites on  
41 orbital prefrontal cortex dopamine axons. In contrast, dopamine innervation to the piriform  
42 cortex is not protracted across adolescence and is not impacted by amphetamine exposure  
43 during adolescence, indicating that dopamine development during adolescence is a uniquely  
44 prefrontal phenomenon. This renders these fibres, and the prefrontal cortex in general,  
45 particularly vulnerable to environmental risk factors during adolescence, such as  
46 recreational drug use.

47

48 **Significance**

49 Dopamine function in the orbital prefrontal cortex underlies many complex cognitive tasks  
50 and is disrupted by drugs of abuse. However, the developmental trajectory of the dopamine  
51 innervation to this portion of the prefrontal cortex remains almost completely unstudied.  
52 We show that dopamine axons continue to innervate the orbital prefrontal cortex during  
53 adolescence. This renders these axons particularly vulnerable to environmental influences.  
54 Exposure to amphetamine, at doses equivalent to those used recreationally by adolescent  
55 people, reduces the number of dopamine connections in the orbital prefrontal cortex. This  
56 effect is selective; it also occurs in the medial prefrontal cortex but not in the piriform  
57 cortex. The impact of amphetamine on cortical dopamine development in adolescence  
58 appears to be a uniquely prefrontal phenomenon.

59

## 60 **1 Introduction**

61 The prefrontal cortex is one of the last brain regions to mature, with changes in structure  
62 and connectivity continuing through adolescence and into early adulthood (Paus, 2005;  
63 Casey et al., 2008; Caballero et al., 2016). In parallel with these changes, higher order  
64 cognitive process that depend on prefrontal cortex function are also maturing (Sturman and  
65 Moghaddam, 2011; Luna et al., 2015; Doremus-Fitzwater and Spear, 2016). Because the  
66 function of the prefrontal cortex is profoundly influenced by the dopamine innervation it  
67 receives (Ranganath and Jacob, 2015; Hoops and Flores, 2017), mesocortical dopamine  
68 development is an important component of this maturational process. However, the  
69 prefrontal cortex is separated into distinct anatomical regions with distinct functions, (Kolb,  
70 2006; Fuster, 2015; Gourley and Taylor, 2016) and our understanding of prefrontal cortex  
71 dopamine development is almost entirely restricted to its medial region (mPFC).

72

73 Dopamine connectivity in the mPFC continues to be established throughout adolescence  
74 and into early adulthood in both rodents and primates (Kalsbeek et al., 1988; Rosenberg and  
75 Lewis, 1995; Benes et al., 2000; Manitt et al., 2011; Naneix et al., 2012; Willing et al., 2017).  
76 In mice, the protracted development of the dopamine input to the mPFC results from the  
77 ongoing growth of dopamine axons during adolescence (Reynolds et al., 2017a). These  
78 axons innervate the nucleus accumbens (NAcc) at the onset of adolescence and grow out of  
79 the NAcc during the adolescent period. They are uniquely vulnerable to environmental  
80 influences during adolescence and exposure to stimulant drugs alters their development, in  
81 part by denuding them of presynaptic sites (Reynolds et al., 2015). These alterations result  
82 in persistent cognitive changes in adulthood  
83 (Reynolds et al., 2015; see also Ye et al., 2014; Kang et al., 2016).

84

85 Whether the dopamine innervation to the orbital prefrontal cortex (oPFC) also continues  
86 through adolescence remains understudied (but see Kalsbeek et al., 1988). In rodents and  
87 primates, the oPFC plays a central role in some of the most complex cognitive functions of  
88 the prefrontal cortex, including decision making, cognitive control, and sociality (Bari and  
89 Robbins, 2013; Pellis and Pellis, 2013; Wilson et al., 2014). Furthermore, exposure to  
90 stimulant drugs alters the structure and function of the oPFC, impacting associated  
91 behaviours (Schoenbaum et al., 2006; Goldstein and Volkow, 2011).

92

93 There is a longstanding controversy surrounding the designation of the prefrontal cortex in  
94 the rodent and whether it is truly homologous to the prefrontal cortex in the primate  
95 (Preuss, 1995; Uylings et al., 2003; Kolb, 2006; Wise, 2008; Carlén, 2017). However,  
96 many characteristics of the prefrontal cortex important to this study, such as its adolescent

97 maturation (Paus, 2005; Casey et al., 2008; Caballero et al., 2016) and the corresponding  
98 changes in cognition and behaviour (Sturman and Moghaddam, 2011; Luna et al., 2015;  
99 Doremus-Fitzwater and Spear, 2016), are shared between rodents and primates.  
100 Furthermore, recent literature supports the hypothesis that the oPFC in particular is  
101 homologous between primates and rodents (Heilbronner et al., 2016; Izquierdo, 2017).

102

103 In this study, we first characterized the adolescent dopamine innervation to the oPFC in  
104 mice. We then examined whether exposure to amphetamine in adolescence affects oPFC  
105 dopamine development. To determine whether the adolescent trajectory of the dopamine  
106 innervation to the prefrontal cortex is unique, we conducted parallel studies in the adjacent  
107 piriform cortex, which is not part of the prefrontal cortex.

108

## 109 **2 Materials & Methods**

110

### 111 **2.1 Animals**

112 Experiments and procedures were performed in accordance with the guidelines of the  
113 [Author University] animal care committee's regulations. Mice were received from Charles  
114 River Canada and housed with same-sex littermates at the [Author University]  
115 Neurophenotyping Centre on a 12h light/dark cycle with *ad libitum* access to food and  
116 water. In this study we define "early adolescence" in C57/BL6 mice as between the weaning  
117 day (post-natal day, PND 21) and PND 32 (Hoops and Flores, 2017). Male mice were used for  
118 all experiments.

119

### 120 **2.2 Drug Administration**

121 d-Amphetamine sulfate (amphetamine; Sigma-Aldrich) was dissolved in 0.9% saline. Mice  
122 were assigned to “drug” and “saline” groups and received one injection of either  
123 amphetamine (dose: 4 mg/kg) or saline via intraperitoneal injection once every other day  
124 for a total of five injections. This treatment regimen was administered during early  
125 adolescence, commencing on PND  $22 \pm 1$  and terminating on PND  $31 \pm 1$ . This regiment has  
126 previously been shown to alter mPFC development when administered in early adolescence  
127 but not adulthood (Reynolds et al., 2015).

128

129 We chose a dose of amphetamine that would achieve a blood plasma concentration in  
130 rodents (Riffée et al., 1978; Feldpausch et al., 1998; Van Swearingen et al., 2013) within the  
131 range of plasma levels achieved by recreational intake of amphetamine in human  
132 adolescents (Kramer et al., 1967; Änggård et al., 1970a; 1970b; Gustavsen et al., 2006).  
133 Blood plasma concentrations of a lipophilic drug in humans and rodents are likely to result  
134 in similar drug concentrations in the brain (Kuczenski and Segal, 2005).

135

### 136 **2.3 Tissue Processing**

137 Mice were euthanized with an intraperitoneal injection of 50 mg/kg ketamine, 5 mg/kg  
138 xylazine, and 1 mg/kg acepromazine. They were then perfused intracardially with 10 IU/mL  
139 heparinized saline followed by 4% paraformaldehyde. Both perfused solutions were pH-  
140 adjusted to between 7.2-7.4 with dilute hydrochloric acid and sodium hydroxide. After  
141 perfusion, brains were dissected from the skull, placed in 4% paraformaldehyde overnight at  
142 4°C, and then stored in phosphate-buffered saline at 4°C. After up to two days in storage,  
143 brains were cut coronally into 35µm thick sections on a vibratome.

144

145 Every second section was processed for immunofluorescence. A polyclonal rabbit anti-  
146 tyrosine hydroxylase (TH; a commonly used marker for dopamine) antibody (Millipore  
147 product #AB152, RRID #AB\_390204, 1:1000 dilution) and an Alexa Fluor (AF) 594-conjugated  
148 polyclonal donkey anti-rabbit antibody (Jackson Laboratories product #711585152, RRID  
149 #AB\_2340621, 1:500 dilution) were used as primary and secondary antibodies. The  
150 manufacturer's certificate of analysis reports that the immunogen for the primary antibody  
151 is denatured TH from rat pheochromocytoma. Its specificity has been verified by Western  
152 blot (Millipore) and immunoprecipitation (Haycock, 1987). The fibres labelled by this  
153 antibody show features indistinguishable from the classic features of cortical dopamine  
154 axons in rodents (Berger et al., 1974; 1983; Van Eden et al., 1987; Manitt et al., 2011),  
155 namely they are thin fibres with irregularly-spaced varicosities, increase in density towards  
156 the deep cortical layers, and are not regularly oriented in relation to the pial surface. This is  
157 in contrast to rodent norepinephrine fibres, which are smooth or beaded in appearance,  
158 relatively thick with regularly spaced varicosities, increase in density towards the shallow  
159 cortical layers, and are in large part oriented either parallel or perpendicular to the pial  
160 surface (Berger et al., 1974; Levitt and Moore, 1979; Berger et al., 1983; Miner et al., 2003).  
161 Furthermore, previous studies in rodents have noted that only norepinephrine cell bodies  
162 are detectable using immunofluorescence for TH, not norepinephrine processes (Pickel et  
163 al., 1975; Verney et al., 1982; Miner et al., 2003), and we did not observe any  
164 norepinephrine-like fibres. After immunofluorescence staining, sections were mounted onto  
165 gel-coated slides and cover-slipped with a DAPI-containing hardset mounting medium  
166 (product #H1500, Vector Laboratories).

167

## 168 **2.4 Axon Tracking**

169 To prove conclusively that the protracted dopamine innervation to the oPFC during  
170 adolescence is due to new axon growth and not the branching of fibres that reached the  
171 oPFC earlier in life, we adapted an axon-initiated viral transduction technique (Beier et al.,  
172 2015) to track the growth of dopamine axons in adolescent mice. Briefly, at PND22 a  
173 retrogradely transported virus expressing Cre recombinase (CAV-Cre BioCampus  
174 Montpellier; Bru et al., 2010) was injected unilaterally at the level of the NAcc. A Cre-  
175 dependent enhanced yellow fluorescent protein (eYFP) virus DIO-eYFP (pAAV-Ef1a-DIO-  
176 EYFP-WPRE-pA, UNC Vector Core) was simultaneously injected into the ipsilateral ventral  
177 tegmental area. CAV-Cre requires the coxsackievirus adenovirus receptor to be taken up  
178 and is therefore preferentially taken up by axon terminals (Bru et al., 2010). This  
179 recombination strategy limits eYFP labeling to ventral tegmental area neurons with axons  
180 that terminate in the NAcc at PND22. Dopamine axons that continue to grow from the NAcc  
181 to the oPFC in adolescence can be detected in adulthood by stereologically counting eYFP-  
182 expressing dopamine varicosities in the oPFC. To rule out the possibility of detecting  
183 dopamine axons in the NAcc that send collaterals to the oPFC, identical dual viral injections  
184 were performed in three adult mice and we counted eYFP-expressing dopamine varicosities  
185 in the oPFC three months later. It is important to note that this virally-mediated axon-  
186 tracking technique only infects a small percentage of ventral tegmental area neurons that  
187 innervate the NAcc (Beier et al., 2015). Therefore, the number of TH+ varicosities in the  
188 adult oPFC that are eYFP+ is an underestimation of the total population of dopamine  
189 varicosities on axons that have grown to the oPFC during adolescence.

190

## 191 **2.5 Stereotaxic surgery**

192 Early adolescent (PND22 ± 1) wild-type mice were anesthetized with isoflurane.  
193 Simultaneous unilateral stereotaxic infusions of DIO-eYFP into the VTA and CAV-Cre into the  
194 NAcc were performed using Hamilton syringe needles. Coordinates were previously verified  
195 by viral and/or dye injection (Manitt et al., 2013; Reynolds et al., 2017b). The coordinates  
196 we used were: VTA: -2.56 mm (anterior/posterior), +0.9 mm (lateral), and -4.1 mm  
197 (dorsal/ventral) relative to Bregma, at a 10° angle; and NAcc: +2.6 mm (anterior/posterior),  
198 +1.5 mm (lateral), and -3.75 mm (dorsal/ventral) relative to Bregma, at a 30° angle. A total  
199 of 0.5 µl of purified virus was delivered over an 8-min period followed by a pause of 6 min.  
200 Adult (PND75 ± 15) wild-type mice underwent the same injection procedure using the  
201 following coordinates: VTA: -3.2 mm (anterior/posterior), +1.0 mm (lateral), and -4.6 mm  
202 (dorsal/ventral) relative to Bregma, at a 10° angle; NAcc: +1.8 mm (anterior/posterior), +3.0  
203 mm (lateral), and -4.8 mm (dorsal/ventral) relative to Bregma, at a 30° angle (Manitt et al.,  
204 2013; Daubaras et al., 2014). Carprofen was delivered subcutaneously during surgery and as  
205 a diet supplement (MediGel CPF, Clear H2O, Portland, ME) throughout recovery for pain  
206 management.

207

## 208 **2.6 Stereological Analyses**

209 Contours of oPFC subregions and the piriform cortex were delineated on sections  
210 corresponding to plates 14-20 of the mouse brain atlas, resulting in delineations on five  
211 sections per region per mouse (Paxinos and Franklin, 2013). We delineated four oPFC  
212 subregions: the dorsal agranular insular prefrontal cortex (daiPFC), the ventral agranular  
213 insular prefrontal cortex (vaiPFC), the lateral oPFC (loPFC), and the ventral oPFC (voPFC)  
214 using landmarks derived from Paxinos & Franklin (2013). While the oPFC is present at more  
215 anterior levels of the mouse brain, dopamine innervation at these levels is practically

216 absent. The medial subregion of the oPFC is only present at these anterior levels and  
217 therefore is not included in our study.

218

219 Previous work in the mPFC that uses similar methods delineates only the dense dopamine  
220 innervation present in the deep cortical layers (Manitt et al., 2011; 2013; Reynolds et al.,  
221 2015). However, the dopamine innervation to the oPFC is diffuse compared to the mPFC  
222 and no clearly demarcated area of dopamine innervation is present. Therefore, in this study  
223 we only estimate the density of dopamine varicosities within each oPFC subregion; we did  
224 not measure the span of the dopamine innervation as we have done previously (Manitt et  
225 al., 2011; 2013).

226

227 Each cortical subregion was traced at x 5 magnification with a Leica DM400B microscope  
228 and Stereoinvestigator software (MicroBrightField). To estimate the number of labelled  
229 varicosities, we used the optical fractionator probe function of Stereoinvestigator. We  
230 counted TH immunolabelled (TH+) and eYFP expressing (eYFP+) varicosities, as well as  
231 double-labelled varicosities, as appropriate for each experiment. Varicosities were defined  
232 as dilated elements associated with axonal processes and were thus only counted if they  
233 were clearly associated with an axon (Parish et al., 2002; Manitt et al., 2011). A grid of 175  
234  $\mu\text{m}^2$  was superimposed on each contour, starting at a random point within the contour.  
235 Unbiased counting frames ( $25 \mu\text{m}^2$ ) were placed in the top left corner of each grid square.  
236 Depending on the area of the region of interest, between ten and thirty-five counting  
237 frames were quantified per delineation. Counting was conducted at x 100 magnification on  
238 every other mounted section using a counting depth of  $10 \mu\text{m}$  and a guard zone of  $5 \mu\text{m}$ .  
239 Section thickness was measured while counting and counts were performed blind by a

240 single individual. To assess the volume of each delineated region we used the Cavalieri  
241 volume estimation method in Stereoinvestigator, with a grid of  $100 \mu\text{m}^2$ . To calculate  
242 varicosity density for each region of interest in each brain, we divided the total varicosity  
243 estimates obtained using the optical fractionator by the estimated volume obtained using  
244 the Cavalieri estimator.

245

246 Varicosities were used as the counting unit to obtain a measure of dopamine presynaptic  
247 density because nearly every dopamine varicosity in the prefrontal cortex forms a synapse  
248 (Séguéla et al., 1988). Varicosities also represent sites where neurotransmitter synthesis,  
249 packaging, release, and reuptake most often occur (Benes et al., 1996). As is standard  
250 practice for our group, we obtained counts only from the right hemisphere.

251

## 252 **2.7 Statistical Analyses**

253 To analyse varicosity density, we conducted two-way mixed ANOVAs with oPFC subregion  
254 and either age (adolescent and adult, result 3.1) or treatment (saline or amphetamine,  
255 result 3.3) as fixed factors, mouse as the random factor, and varicosity density as the  
256 response variable. Each age and treatment group had a sample size of four mice.  
257 Subsequently, we conducted Student's t-tests, corrected for multiple comparisons using the  
258 Hochberg-Bonferroni procedure (Hochberg, 1988), between treatment groups separately  
259 for each oPFC subregion in all cases where either subregion or the interaction term was  
260 significant in the ANOVA. We analysed data for the piriform cortex independently using  
261 Student's t-tests. All data used in this study are available as extended data.

262

## 263 **3 Results**

264 **3.1 Dopamine innervation to the oPFC is protracted across adolescence**

265 We found that the density of dopamine varicosities in the oPFC is significantly higher in  
266 adult mice compared to adolescent mice, indicating that dopamine innervation continues to  
267 increase in the oPFC during adolescence (Figure 1; Extended Data 1-1; two-way ANOVA,  
268 main effect of age,  $F_{(1,18)}=9.904$ ,  $p=0.019$ , no significant effect of region,  $F_{(3,18)}=1.30$ ,  
269  $p=0.305$ , or age  $\times$  region interaction,  $F_{(3,18)}=2.47$ ,  $p=0.095$ ). Post-hoc Hochberg-corrected t-  
270 tests revealed that dopamine innervation increases during adolescence in the loPFC  
271 ( $t_6=3.091$ ,  $p=0.021$ ), daiPFC ( $t_6=3.062$ ,  $p=0.022$ ), and vaiPFC ( $t_6=6.282$ ,  $p=0.0008$ ), but not in  
272 the voPFC ( $t_6=1.495$ ,  $p=0.186$ ). Visual comparison of densities between adolescence and  
273 adulthood in the voPFC (Figure 1e) indicates that high within-group variability underlies the  
274 nonsignificant p-value in the voPFC.

275

276 **3.2 Delayed dopamine innervation to the oPFC results from ongoing axon growth**

277 The axon-initiated recombination technique we used limits eYFP expression to ventral  
278 tegmental area neurons with axons that have reached the NAcc by the start of adolescence  
279 (Beier et al., 2015; Reynolds et al., 2017a). If the axons of these neurons continue to grow to  
280 the oPFC during adolescence, we should observe eYFP-positive dopamine varicosities in the  
281 adult oPFC. Remarkably, we find eYFP dopamine varicosities in all four oPFC subregions in  
282 adult mice that received dual viral infection in early adolescence (Figure 2; Extended Data 2-  
283 1). The presence of these varicosities indicates that dopamine axons indeed continue to  
284 grow to the oPFC from the NAcc during adolescence. To exclude the possibility that these  
285 eYFP-positive dopamine varicosities are collaterals of fibers innervating the NAcc, we  
286 performed the same axon-initiated viral tracing experiment in adult mice. eYFP-positive  
287 dopamine varicosities in the oPFC are absent or negligible in these mice (Figure 2; Extended

288 Data 2-1).

289

### 290 **3.3 Amphetamine in adolescence reduces dopamine varicosity density in the adult oPFC**

291 Amphetamine in adolescence has been found to reduce the number of presynaptic sites  
292 from mPFC dopamine axons, measured as a significant reduction in dopamine varicosity  
293 density (Reynolds et al., 2015). Here we measured the density of dopamine varicosities in  
294 the oPFC in adult mice exposed to the exact same regimen of amphetamine or saline in  
295 adolescence as in Reynolds et al. (2015). Similar to the mPFC, amphetamine in adolescence  
296 results in significantly fewer dopamine varicosities in the oPFC (Figure 3; Extended Data 3-1;  
297 two-way ANOVA, main effect of age,  $F_{(1,12)}=15.12$ ,  $p=0.008$ , no significant effect of region,  
298  $F_{(2,12)}=0.42$ ,  $p=0.670$ , or age  $\times$  region interaction,  $F_{(2,12)}=3.68$ ,  $p=0.057$ ). Post-hoc Hochberg-  
299 corrected t-tests revealed that dopamine varicosities were reduced in the daiPFC ( $t_6=4.987$ ,  
300  $p=0.003$ ) and vaiPFC ( $t_6=3.630$ ,  $p=0.011$ ), while the effect in the loPFC was marginal  
301 ( $t_6=2.370$ ,  $p=0.056$ ).

302

### 303 **3.4 Dopamine innervation to the piriform cortex is not protracted nor influenced by** 304 **amphetamine in adolescence**

305 We measured dopamine varicosity density in the piriform cortex, a cortical region that is not  
306 part of the prefrontal cortex, in adolescent and adult mice. In contrast to the mPFC  
307 (Kalsbeek et al., 1988) and oPFC, dopamine varicosity density in the piriform cortex is  
308 significantly higher in adolescence compared to adulthood (Figure 4; Extended Data 4-1;  
309  $t_6=8.256$ ,  $p=0.0002$ ).

310

311 In addition, amphetamine during adolescence does not alter dopamine varicosity density:

312 levels are similar between adult mice treated with drug or saline in adolescence (Figure 4;  
313 Extended Data 4-2;  $t_6=0.7985$ ,  $p=0.455$ ). This indicates that it is specifically the dopamine  
314 innervation to the prefrontal cortex that is sensitive to amphetamine during adolescence.  
315

#### 316 **4 Discussion**

317 The increase in mPFC dopamine innervation during adolescence is a well-known  
318 phenomenon, both in rodents and primates (Kalsbeek et al., 1988; Rosenberg and Lewis,  
319 1995; Benes et al., 2000; Manitt et al., 2011; Naneix et al., 2012; Willing et al., 2017;  
320 Reynolds et al., 2017a). However, until now adolescent dopamine innervation in the oPFC  
321 remained almost completely unstudied (but see Kalsbeek et al., 1988). Here, we show that  
322 in mice the dopamine innervation to the oPFC is still maturing during adolescence.  
323 Specifically, oPFC dopamine varicosity density increases during this period. Critically, this  
324 increase is due to the growth of new axons to the oPFC. Because oPFC dopamine axons are  
325 still growing, they remain vulnerable to environmental influences for an extended  
326 spatiotemporal window. We find that exposure to amphetamine during adolescence  
327 reduces the number of dopamine varicosities in the oPFC in adulthood. Notably, these  
328 effects appear to be specific to the prefrontal cortex; we do not find them in the adjacent  
329 piriform cortex.

330

331 Though we discuss our findings in the context of the relevant literature, we note that the  
332 matter of prefrontal cortex homology between the rodent and primate is not yet settled  
333 (Carlén, 2017). However, available evidence strongly supports homology between the  
334 rodent and primate oPFC (Uylings et al., 2003; Heilbronner et al., 2016; Izquierdo,  
335 2017). Finally, homology between the primate and rodent oPFC would imply that the oPFC

336 is homologous amongst rodents, however to our knowledge there are no studies directly  
337 examining this. Therefore, we encourage caution in translating our findings to other  
338 rodents, including rats.

339

340 The Netrin-1 receptor DCC is responsible for coordinating dopamine axon structure and  
341 function in the mPFC (Hoops and Flores, 2017). Reducing DCC expression on ventral  
342 tegmental neurons in adolescence induces structural deficiencies in mPFC dopamine axons  
343 (Reynolds et al., 2017a), and amphetamine in adolescence reduces DCC expression on these  
344 neurons (Yetnikoff et al., 2010; 2011). These alterations result in persistent cognitive  
345 changes in adulthood (Reynolds et al., 2015). Our results suggest that amphetamine in  
346 adolescence is reducing DCC expression on ventral tegmental dopamine neurons that  
347 project to the oPFC, resulting in denuded dopamine axons in this region. Furthermore, since  
348 the vast majority of dopamine varicosities form synapses (Séguéla et al., 1988), the  
349 reduction we see in varicosities in amphetamine-treated mice suggests that dopamine  
350 axons are forming far fewer synapses in the oPFC as compared to mice treated with saline.  
351 Therefore, our results suggest that the growing dopamine axons are vulnerable to  
352 environmental influences and that amphetamine exposure during adolescence may impair  
353 the formation of dopamine synapses onto their target cells within the oPFC.

354

355 The piriform cortex, part of the mammalian olfactory cortex, is structurally and functionally  
356 linked to the oPFC in rodents and humans (Gottfried et al., 2003; Uylings et al., 2003; Fuster,  
357 2015) and in rodents receives about the same density of dopamine input as the oPFC (Fallon  
358 and Loughlin, 1987). However, unlike the oPFC, the piriform cortex matures relatively early  
359 in human postnatal development (Gogtay et al., 2004; Shaw et al., 2008), as do piriform

360 cortex-dependent olfactory discrimination behaviours in rodents (Staubli et al., 1987; Hu et  
361 al., 1997). Therefore, the piriform cortex was an ideal cortical region to use to examine  
362 whether our results are specific to the prefrontal cortex or reflect general trends in frontal  
363 cortex development. To our knowledge, this is the first time that the postnatal  
364 developmental time course of the dopamine innervation to the piriform cortex has been  
365 studied, and so we feel that our findings in this region are also important in their own right.  
366 We find that adolescent mice had a higher density of dopamine varicosities compared to  
367 adult mice, the opposite pattern to the one we observed in the oPFC. However, this result is  
368 in line with what is observed in the cortex as a whole, where there is an overproduction of  
369 synapses during early adolescence followed by a period of rapid pruning in primates and  
370 rodents (Lidow et al., 1991; Andersen, 2003; Crews et al., 2007; Juraska and Willing, 2017).  
371 In fact, it has been estimated that in primates as many as 30 000 synapses may be lost per  
372 second over the entire cortex during adolescence, resulting in an overall loss of up to one  
373 half the total number of synapses present during early adolescence (Rakic et al., 1994). Our  
374 findings are also in line with a study that found dopamine receptor expression in the rat  
375 piriform cortex peaks in adolescence before declining in adulthood (Garske et al., 2013).  
376 Therefore, axon growth and synapse formation during adolescence appears to be a unique  
377 characteristic of the mesocortical dopamine projections to the prefrontal cortex.

378

### 379 **5 Conclusion**

380 Taken together, our results show that dopamine development to the oPFC is delayed across  
381 adolescence. Importantly, we have found that this delayed growth is due to axons that  
382 previously innervated the nucleus accumbens leaving this region and growing to the oPFC  
383 during this period. Furthermore, we show that these axons are vulnerable to environmental

384 influences such as exposure to addictive drugs. Amphetamine exposure during early  
385 adolescence results in reduced synapse formation in the oPFC. Finally, dopamine  
386 innervation to the piriform cortex reaches adult densities prior to adolescence, indicating  
387 that delayed growth of dopamine axons, and the associated vulnerability to environmental  
388 influences, is specific to the prefrontal cortex.

389

## 390 **6 References**

- 391 Andersen SL (2003) Trajectories of brain development: point of vulnerability or window of  
392 opportunity? *Neurosci Biobehav Rev* 27:3–18.
- 393 Änggård E, Gunne LM, Jönsson LE, Niklasson F (1970a) Pharmacokinetic and clinical studies  
394 on amphetamine dependent subjects. *Eur J Clin Pharmacol* 3:3–11.
- 395 Änggård E, Gunne LM, Niklasson F (1970b) Gas Chromatographic Determination of  
396 Amphetamine in Blood, Tissue, and Urine. *Scand J Clin Lab Invest* 26:137–143.
- 397 Bari A, Robbins TW (2013) Inhibition and impulsivity: Behavioral and neural basis of  
398 response control. *Prog Neurobiol* 108:44–79.
- 399 Beier KT, Steinberg EE, DeLoach KE, Xie S, Miyamichi K, Schwarz L, Gao XJ, Kremer EJ,  
400 Malenka RC, Luo L (2015) Circuit Architecture of VTA Dopamine Neurons Revealed by  
401 Systematic Input-Output Mapping. *Cell* 162:622–634.
- 402 Benes FM, Taylor JB, Cunningham MC (2000) Convergence and plasticity of monoaminergic  
403 systems in the medial prefrontal cortex during the postnatal period: implications for the  
404 development of psychopathology. *Cereb Cortex* 10:1014–1027.
- 405 Benes FM, Vincent SL, Molloy R, Khan Y (1996) Increased interaction of dopamine-  
406 immunoreactive varicosities with GABA neurons of rat medial prefrontal cortex occurs  
407 during the postweanling period. *Synapse* 23:237–245.
- 408 Berger B, Tassin JP, Blanc G, Moyne MA, Thierry AM (1974) Histochemical confirmation for  
409 dopaminergic innervation of the rat cerebral cortex after destruction of the  
410 noradrenergic ascending pathways. *Brain Res* 81:332–337.
- 411 Berger B, Verney C, Gay M, Vigny A (1983) Immunocytochemical Characterization of the  
412 Dopaminergic and Noradrenergic Innervation of the Rat Neocortex During Early  
413 Ontogeny. In: *Proceedings of the 9th Meeting of the International Neurobiology Society*,  
414 pp 263–267 *Progress in Brain Research*. Elsevier.
- 415 Bru T, Salinas S, Kremer EJ (2010) An Update on Canine Adenovirus Type 2 and Its Vectors.  
416 *Viruses* 2010, Vol 2, Pages 2134–2153 2:2134–2153.

- 417 Caballero A, Granberg R, Tseng KY (2016) Mechanisms contributing to prefrontal cortex  
418 maturation during adolescence. *Neurosci Biobehav Rev* 70:4–12.
- 419 Carlén M (2017) What constitutes the prefrontal cortex? *Science* 358:478–482.
- 420 Casey BJ, Jones RM, Hare TA (2008) The Adolescent Brain. *Ann N Y Acad Sci* 1124:111–126.
- 421 Crews FT, He J, Hodge C (2007) Adolescent cortical development: a critical period of  
422 vulnerability for addiction. *Pharmacol Biochem Behav* 86:189–199.
- 423 Daubaras M, Dal Bo G, Flores C (2014) Target-dependent expression of the netrin-1  
424 receptor, UNC5C, in projection neurons of the ventral tegmental area. *Neurosci* 260:36–  
425 46 Available at: <http://dx.doi.org/10.1016/j.neuroscience.2013.12.007>.
- 426 Doremus-Fitzwater TL, Spear LP (2016) Reward-centricity and attenuated aversions: An  
427 adolescent phenotype emerging from studies in laboratory animals. 70:121–134.
- 428 Fallon JH, Loughlin SE (1987) Monoamine innervation of cerebral cortex and a theory of the  
429 role of monoamines in cerebral cortex and basal ganglia. *Cereb Cortex*:41–127.
- 430 Feldpausch DL, Needham LM, Stone MP, Althaus JS, Yamamoto BK, Svensson KA, Merchant  
431 KM (1998) The role of dopamine D4 receptor in the induction of behavioral sensitization  
432 to amphetamine and accompanying biochemical and molecular adaptations. *J*  
433 *Pharmacol Exp Ther* 286:497–508.
- 434 Fuster JM (2015) *The Prefrontal Cortex*, 5 ed. Elsevier.
- 435 Garske AK, Lawyer CR, Peterson BM, Illig KR (2013) Adolescent Changes in Dopamine D1  
436 Receptor Expression in Orbitofrontal Cortex and Piriform Cortex Accompany an  
437 Associative Learning Deficit Ravel N, ed. *PLoS ONE* 8:e56191.
- 438 Gogtay N, Giedd JN, Lusk L, Hayashi KM, Greenstein D, Vaituzis AC, Nugent TF, Herman DH,  
439 Clasen LS, Toga AW, Rapoport JL, Thompson PM (2004) Dynamic mapping of human  
440 cortical development during childhood through early adulthood. *PNAS* 101:8174–8179.
- 441 Goldstein RZ, Volkow ND (2011) Dysfunction of the prefrontal cortex in addiction:  
442 neuroimaging findings and clinical implications. *Nat Rev Neurosci* 12:nrn3119–nrn3669  
443 Available at: <http://dx.doi.org/10.1038/nrn3119>.
- 444 Gottfried JA, O'Doherty J, Dolan RJ (2003) Encoding Predictive Reward Value in Human  
445 Amygdala and Orbitofrontal Cortex. *Science* 301:1104–1107.
- 446 Gourley SL, Taylor JR (2016) Going and stopping: dichotomies in behavioral control by the  
447 prefrontal cortex. *Nat Neurosci* 19:656–664.
- 448 Gustavsen I, Mørland J, Bramness JG (2006) Impairment related to blood amphetamine  
449 and/or methamphetamine concentrations in suspected drugged drivers. *Accident*  
450 *Analysis & Prevention* 38:490–495.
- 451 Haycock JW (1987) Stimulation-Dependent phosphorylation of tyrosine hydroxylase in rat

- 452 corpus striatum. *Brain Res Bull* 19:619–622.
- 453 Heilbronner SR, Rodriguez-Romaguera J, Quirk GJ, Groenewegen HJ, Haber SN (2016)  
454 Circuit-Based Corticostriatal Homologies Between Rat and Primate. *Biol Psych* 80:509–  
455 521 Available at: <http://dx.doi.org/10.1016/j.biopsych.2016.05.012>.
- 456 Hochberg Y (1988) A sharper Bonferroni procedure for multiple tests of significance.  
457 *Biometrika* 75:800–802.
- 458 Hoops D, Flores C (2017) Making Dopamine Connections in Adolescence. *Trends Neurosci*:1–  
459 11.
- 460 Hu D, Griesbach G, Amsel A (1997) Development of vicarious trial-and-error behavior in  
461 odor discrimination learning in the rat: relation to hippocampal function? *Behav Brain*  
462 *Res* 86:67–70.
- 463 Izquierdo A (2017) Functional Heterogeneity within Rat Orbitofrontal Cortex in Reward  
464 Learning and Decision Making. *J Neurosci* 37:10529–10540.
- 465 Juraska JM, Willing J (2017) Pubertal onset as a critical transition for neural development  
466 and cognition. *Brain Res* 1654:87–94 Available at:  
467 <http://linkinghub.elsevier.com/retrieve/pii/S0006899316302050>.
- 468 Kalsbeek A, Voorn P, Buijs RM, Pool CW, Uylings HBM (1988) Development of the  
469 Dopaminergic Innervation in the Prefrontal Cortex of the Rat. *J Comp Neurol* 269:58–72.
- 470 Kang S, Wu MM, Galvez R, Gulley JM (2016) Timing of amphetamine exposure in relation to  
471 puberty onset determines its effects on anhedonia, exploratory behavior, and dopamine  
472 D1 receptor expression in young adulthood. *Neurosci* 339:72–84.
- 473 Kolb B (2006) Do all mammals have a prefrontal cortex? In: *Evolution of Nervous Systems: A*  
474 *Comprehensive Reference; Four-Volume Set*, pp 443–450. Academic Press.
- 475 Kramer JC, Fischman VS, Littlefield DC (1967) Amphetamine Abuse: Pattern and Effects of  
476 High Doses Taken Intravenously. *JAMA* 201:305–309.
- 477 Kuczenski R, Segal DS (2005) Stimulant Actions in Rodents: Implications for Attention-  
478 Deficit/Hyperactivity Disorder Treatment and Potential Substance Abuse. *Biol Psych*  
479 57:1391–1396.
- 480 Levitt P, Moore RY (1979) Development of the noradrenergic innervation of neocortex.  
481 *Brain Res* 162:243–259.
- 482 Lidow MS, Goldman-Rakic PS, Rakic P (1991) Synchronized overproduction of  
483 neurotransmitter receptors in diverse regions of the primate cerebral cortex. *PNAS*  
484 88:10218–10221.
- 485 Luna B, Marek S, Larsen B, Tervo-Clemmens B, Chahal R (2015) An integrative model of the  
486 maturation of cognitive control. *Annu Rev Neurosci* 38:151–170.

- 487 Manitt C et al. (2013) dcc orchestrates the development of the prefrontal cortex during  
488 adolescence and is altered in psychiatric patients. *Transl Psychiatry* 3:e338–13.
- 489 Manitt C, Mimee A, Eng C, Pokinko M, Stroh T, Cooper HM, Kolb B, Flores C (2011) The  
490 Netrin Receptor DCC Is Required in the Pubertal Organization of Mesocortical Dopamine  
491 Circuitry. *J Neurosci* 31:8381–8394.
- 492 Miner LH, Schroeter S, Blakely RD, Sesack SR (2003) Ultrastructural localization of the  
493 norepinephrine transporter in superficial and deep layers of the rat prelimbic prefrontal  
494 cortex and its spatial relationship to probable dopamine terminals. *J Comp Neurol*  
495 466:478–494.
- 496 Naneix F, Marchand AR, Di Scala G, Pape JR, Coutureau E (2012) Parallel Maturation of Goal-  
497 Directed Behavior and Dopaminergic Systems during Adolescence. *J Neurosci* 32:16223–  
498 16232.
- 499 Parish CL, Stanic D, Drago J, Borrelli E, Finkelstein DI, Horne MK (2002) Effects of long-term  
500 treatment with dopamine receptor agonists and antagonists on terminal arbor size. *Eur*  
501 *J Neurosci* 16:787–794.
- 502 Paus T (2005) Mapping brain maturation and cognitive development during adolescence.  
503 *Trends Cogn Sci* 9:60–68 Available at:  
504 <http://linkinghub.elsevier.com/retrieve/pii/S1364661304003201>.
- 505 Paxinos G, Franklin KBJ (2013) The mouse brain in stereotaxic coordinates. Academic Press.
- 506 Pellis S, Pellis V (2013) The Playful Brain. Oneworld Publications.
- 507 Pickel VM, Joh TH, Field PM, Becker CG, Reis DJ (1975) Cellular localization of tyrosine  
508 hydroxylase by immunohistochemistry. *J Histochem Cytochem* 23:1–12.
- 509 Preuss TM (1995) Do rats have prefrontal cortex? The rose-woolsey-akert program  
510 reconsidered. *J Cogn Neurosci* 7:1–24.
- 511 Rakic P, Bourgeois J-P, Goldman-Rakic PS (1994) Synaptic development of the cerebral  
512 cortex: implications for learning, memory, and mental illness. In: *The Self-Organizing*  
513 *Brain: From Growth Cones to Functional Networks*, pp 227–243 *Progress in Brain*  
514 *Research*. Elsevier.
- 515 Ranganath A, Jacob SN (2015) Doping the Mind. *The Neuroscientist* 22:593–603.
- 516 Reynolds LM, Makowski CS, Yogendran SV, Kiessling S, Cermakian N, Flores C (2015)  
517 Amphetamine in Adolescence Disrupts the Development of Medial Prefrontal Cortex  
518 Dopamine Connectivity in a dcc-Dependent Manner. *Neuropsychopharmacology*  
519 40:1101–1112.
- 520 Reynolds LM, Pokinko M, Torres-Berrío A, Cuesta S, Lambert LC, Del Cid Pellitero E,  
521 Wodzinski M, Manitt C, Krimpenfort P, Kolb B, Flores C (2017a) DCC Receptors Drive  
522 Prefrontal Cortex Maturation by Determining Dopamine Axon Targeting in Adolescence.  
523 *Biol Psych*.

- 524 Reynolds LM, Pokinko M, Torres-Berrío A, Cuesta S, Lambert LC, Del Cid Pellitero E,  
525 Wodzinski M, Manitt C, Krimpenfort P, Kolb B, Flores C (2017b) DCC Receptors Drive  
526 Prefrontal Cortex Maturation by Determining Dopamine Axon Targeting in Adolescence.  
527 Biol Psych.
- 528 Riffée WH, Ludden TM, Wilcox RE, Gerald MC (1978) Brain and plasma concentrations of  
529 amphetamine isomers in mice. *J Pharmacol Exp Ther* 206:586–594.
- 530 Rosenberg DR, Lewis DA (1995) Postnatal Maturation of the Dopaminergic Innervation of  
531 Monkey Prefrontal and Motor Cortices - a Tyrosine-Hydroxylase Immunohistochemical  
532 Analysis. *J Comp Neurol* 358:383–400.
- 533 Schoenbaum G, Roesch MR, Stalnaker TA (2006) Orbitofrontal cortex, decision-making and  
534 drug addiction. *Trends Neurosci* 29:116–124.
- 535 Séguéla P, Watkins KC, Descarries L (1988) Ultrastructural features of dopamine axon  
536 terminals in the anteromedial and the suprarhinal cortex of adult rat. *Brain Res* 442:11–  
537 22.
- 538 Shaw PW, Kabani NJ, Lerch JP, Eckstrand K, Lenroot R, Gogtay N, Greenstein D, Clasen L,  
539 Evans A, Rapoport JL, Giedd JN, Wise SP (2008) Neurodevelopmental Trajectories of the  
540 Human Cerebral Cortex. *J Neurosci* 28:3586–3594.
- 541 Staubli U, Schottler F, Nejat-Bina D (1987) Role of dorsomedial thalamic nucleus and  
542 piriform cortex in processing olfactory information. *Behav Brain Res* 25:117–129.
- 543 Sturman DA, Moghaddam B (2011) The neurobiology of adolescence: Changes in brain  
544 architecture, functional dynamics, and behavioral tendencies. 35:1704–1712.
- 545 Uylings HBM, Groenewegen HJ, Kolb B (2003) Do rats have a prefrontal cortex? *Behav Brain*  
546 *Res* 146:3–17.
- 547 Van Eden CG, Hoorneman EM, Buijs RM, Matthijssen MA, Geffard M, Uylings HBM (1987)  
548 Immunocytochemical localization of dopamine in the prefrontal cortex of the rat at the  
549 light and electron microscopical level. *Neurosci* 22:849–862.
- 550 Van Swearingen AED, Walker QD, Kuhn CM (2013) Sex differences in novelty- and  
551 psychostimulant-induced behaviors of C57BL/6 mice. *Psychopharmacology* 225:707–  
552 718.
- 553 Verney C, Berger B, Adrien J, Vigny A, Gay M (1982) Development of the dopaminergic  
554 innervation of the rat cerebral cortex. A light microscopic immunocytochemical study  
555 using anti-tyrosine hydroxylase antibodies. *Dev Brain Res* 5:41–52.
- 556 Willing J, Cortes LR, Brodsky JM, Kim T, Juraska JM (2017) Innervation of the medial  
557 prefrontal cortex by tyrosine hydroxylase immunoreactive fibers during adolescence in  
558 male and female rats. *Dev Psychobiol* 59:583–589.
- 559 Wilson RC, Takahashi YK, Schoenbaum G, Niv Y (2014) Orbitofrontal cortex as a cognitive  
560 map of task space. *Neuron* 81:267–279.

- 561 Wise SP (2008) Forward frontal fields: phylogeny and fundamental function. Trends  
562 Neurosci 31:599–608.
- 563 Ye T, Pozos H, Phillips TJ, Izquierdo A (2014) Long-term effects of exposure to  
564 methamphetamine in adolescent rats. Drug and Alcohol Dependence 138:17–23.
- 565 Yetnikoff L, Almey A, Arvanitogiannis A, Flores C (2011) Abolition of the behavioral  
566 phenotype of adult netrin-1 receptor deficient mice by exposure to amphetamine  
567 during the juvenile period. Psychopharmacology 217:505–514.
- 568 Yetnikoff L, Eng C, Benning S, Flores C (2010) Netrin-1 receptor in the ventral tegmental area  
569 is required for sensitization to amphetamine. Eur J Neurosci 31:1292–1302.

570

571 **Figure Captions**

572 **Figure 1.** Dopamine varicosity density in the orbital prefrontal cortex is protracted across  
573 adolescence. (a) Timeline of experimental procedures. n = 4 per group (b) A micrograph of a  
574 coronal section through the frontal cortex of an adult mouse at low magnification (x4)  
575 showing the contour of the orbital prefrontal cortex. scale bar = 500  $\mu\text{m}$  (c) A micrograph of  
576 a coronal section of the orbital prefrontal cortex of an adult mouse at high magnification  
577 (x60) showing tyrosine hydroxylase-immunopositive varicosities. scale bar = 10  $\mu\text{m}$  (d) The  
578 voPFC, loPFC, aivPFC, and aidPFC, respectively, are highlighted in increasingly pale shades of  
579 purple. Line drawings were derived from (Paxinos and Franklin, 2013). (e) Stereological  
580 quantification of dopamine varicosity density reveals that there are more dopamine  
581 varicosities in the adult orbital prefrontal cortex than the adolescent (Data: Figure 1-1).  
582 daiPFC = dorsal agranular insular prefrontal cortex, loPFC = lateral orbital prefrontal cortex,  
583 PND = post-natal day, TH = tyrosine hydroxylase, vaiPFC = ventral agranular insular  
584 prefrontal cortex, voPFC = ventral orbital prefrontal cortex

585

586 **Figure 2.** Axons continue to grow to the orbital prefrontal cortex during adolescence. (a) The  
587 dual-viral injection method used to label NAcc-projecting ventral tegmental area neurons

588 with eYFP. (b) Timeline of experimental procedures: mice were injected at the start of  
589 adolescence (PND22±1) and six weeks later, at which point adolescent mice have reached  
590 adulthood, eYFP-expressing dopamine axons in the oPFC were quantified. n = 5 (c-e)  
591 Micrographs of a coronal section of the orbital prefrontal cortex of an adult mouse at high  
592 magnification (x60) show (c) tyrosine hydroxylase-immunopositive varicosities, (d) eYFP-  
593 expressing varicosities, and (e) an overlay highlighting co-labelled varicosities. scale bar = 10  
594 µm (f) The voPFC, loPFC, aivPFC, and aidPFC, respectively, are highlighted in increasingly  
595 pale shades of purple. Line drawings were derived from (Paxinos and Franklin, 2013). (g)  
596 Stereological quantification of dopamine varicosity density reveals eYFP-expressing  
597 dopamine varicosities are present in the orbital prefrontal cortex in adult mice that received  
598 dual-viral injections in early adolescence (Data: Figure 2-1). (h) To ensure the eYFP-  
599 expressing dopamine neurons in the oPFC were the result of axon growth and not  
600 collaterals, we injected viruses into early adult mice and quantified eYFP-expressing  
601 dopamine axons six weeks later. n = 3 (i) eYFP-expressing dopamine varicosities are almost  
602 entirely absent from the orbital prefrontal cortices of mice that were injected during  
603 adulthood (Data: Figure 2-1). daiPFC = dorsal agranular insular prefrontal cortex, eYFP =  
604 enhanced yellow fluorescent protein, loPFC = lateral orbital prefrontal cortex, PND = post-  
605 natal day, TH = tyrosine hydroxylase, vaiPFC = ventral agranular insular prefrontal cortex,  
606 voPFC = ventral orbital prefrontal cortex

607

608 **Figure 3.** Amphetamine in adolescence alters dopamine connectivity in adulthood. (a)  
609 Timeline of experimental procedures. n = 4 per group (b) The loPFC, aivPFC, and aidPFC,  
610 respectively, are highlighted in increasingly pale shades of red. Line drawings were derived  
611 from (Paxinos and Franklin, 2013). (c) Stereological quantification of dopamine varicosity

612 density reveals that adults exposed to amphetamine during adolescence have about a 40%  
613 reduction in dopamine varicosity density in the oPFC compared to saline-treated controls  
614 (Data: Figure 3-1). daiPFC = dorsal agranular insular prefrontal cortex, loPFC = lateral orbital  
615 prefrontal cortex, PND = post-natal day, TH = tyrosine hydroxylase, vaiPFC = ventral  
616 agranular insular prefrontal cortex

617

618 **Figure 4.** Dopamine connectivity in the piriform cortex is not protracted nor influenced by  
619 amphetamine in adolescence. (a) The piriform cortex was outlined based on Paxinos and  
620 Watson (2013) and is highlighted in purple. (b-c) Stereological quantification of dopamine  
621 varicosity density reveals that (b) early adolescent mice have a significantly higher density of  
622 dopamine varicosities in the piriform cortex compared to adults (Data: Figure 4-1). and (c)  
623 that amphetamine exposure during adolescence does not alter the density of dopamine  
624 varicosities in the piriform cortex (Data: Figure 4-2).

625

#### 626 **Extended Data Captions**

627 **Figure 1-1.** Dopamine (tyrosine hydroxylase immunopositive) varicosity density estimates  
628 for four subregions of the orbital prefrontal cortex in adult and early adolescent mice.  
629 Varicosity density was estimated by combining the optical fractionator and Cavalieri  
630 estimator methods of the software program Stereoinvestigator (see Methods). This data  
631 was used to generate the results presented in Results section 3.1 and Figure 1. daiPFC =  
632 dorsal agranular insular prefrontal cortex, loPFC = lateral orbital prefrontal cortex, vaiPFC =  
633 ventral agranular insular prefrontal cortex

634

635 **Figure 2-1.** Density estimates of dopamine (tyrosine hydroxylase; TH immunopositive)

636 varicosities that have been infected with a fluorescent protein-expressing virus for four  
637 subregions of the orbital prefrontal cortex in adult and early adolescent mice. Varicosity  
638 density was estimated by combining the optical fractionator and Cavalieri estimator  
639 methods of the software program Stereoinvestigator (see Methods). This data was used to  
640 generate the results presented in Results section 3.2 and Figure 2. daiPFC = dorsal agranular  
641 insular prefrontal cortex, eYFP= enhanced yellow fluorescent protein, loPFC = lateral orbital  
642 prefrontal cortex, vaiPFC = ventral agranular insular prefrontal cortex

643

644 **Figure 3-1.** Dopamine (tyrosine hydroxylase immunopositive) varicosity density estimates in  
645 four subregions of the orbital prefrontal cortex in adult mice treated with either saline or  
646 amphetamine in early adolescence. Varicosity density was estimated by combining the  
647 optical fractionator and Cavalieri estimator methods of the software program  
648 Stereoinvestigator (see Methods). This data was used to generate the results presented in  
649 Results section 3.3 and Figure 3. daiPFC = dorsal agranular insular prefrontal cortex, loPFC =  
650 lateral orbital prefrontal cortex, vaiPFC = ventral agranular insular prefrontal cortex

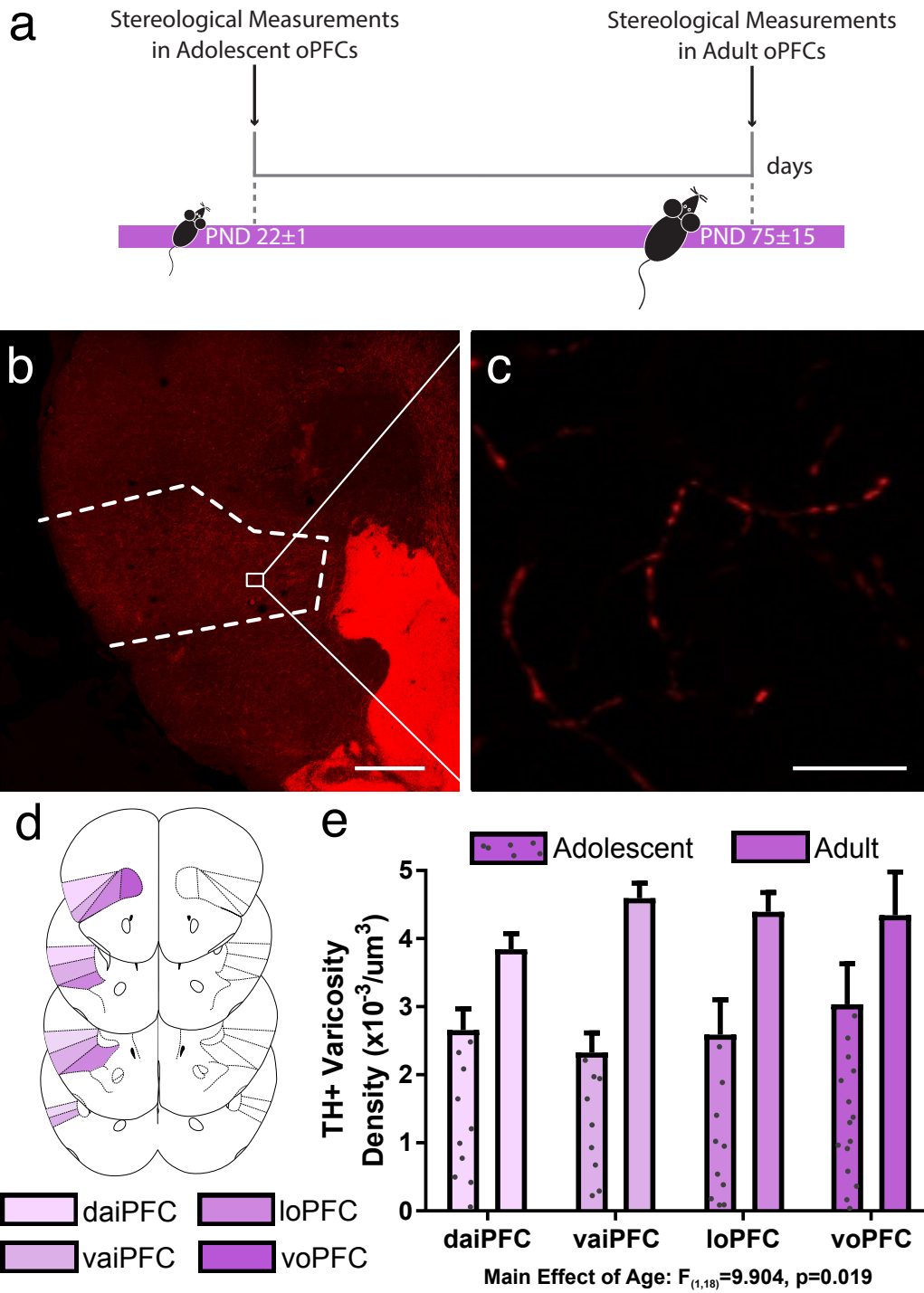
651

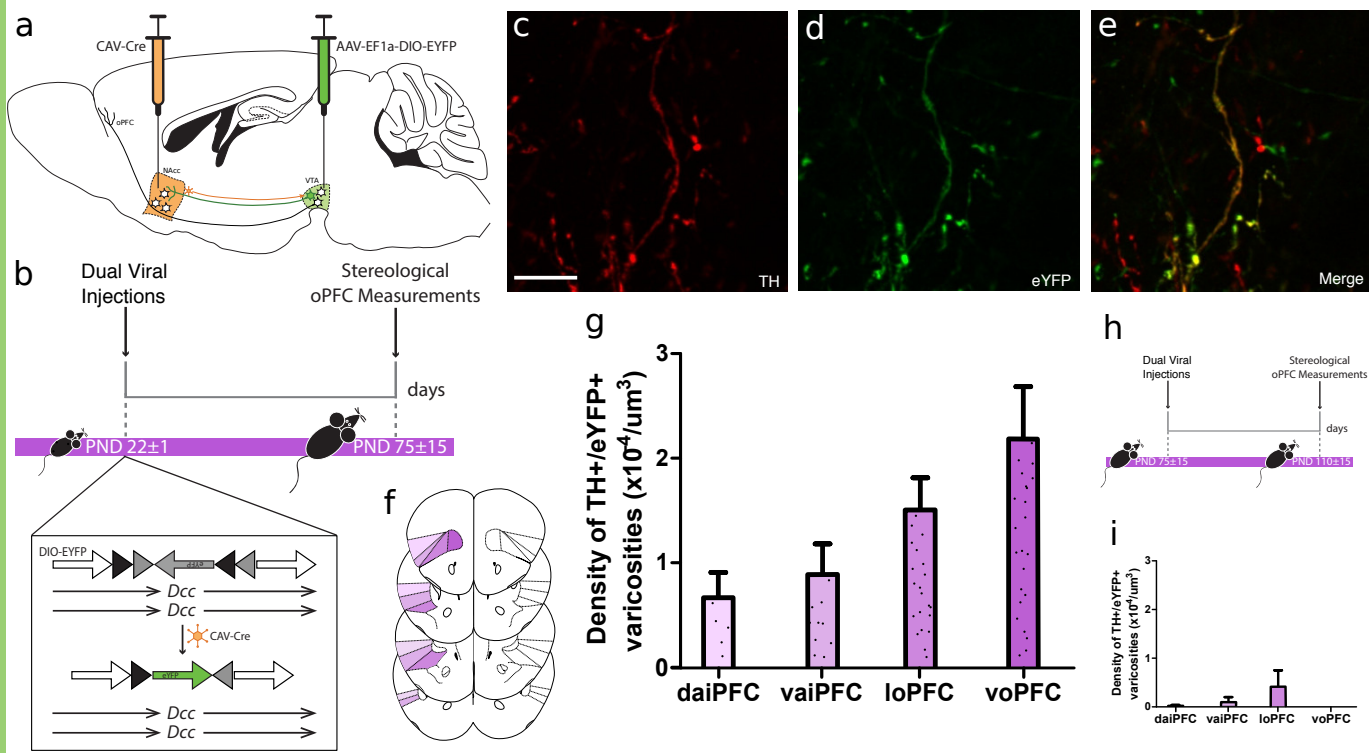
652 **Figure 4-1.** Dopamine (tyrosine hydroxylase immunopositive) varicosity density estimates  
653 for the piriform cortex in adult and early adolescent mice. Varicosity density was estimated  
654 by combining the optical fractionator and Cavalieri estimator methods of the software  
655 program Stereoinvestigator (see Methods). This data was used to generate the results  
656 presented in Results section 3.4 and Figure 4b.

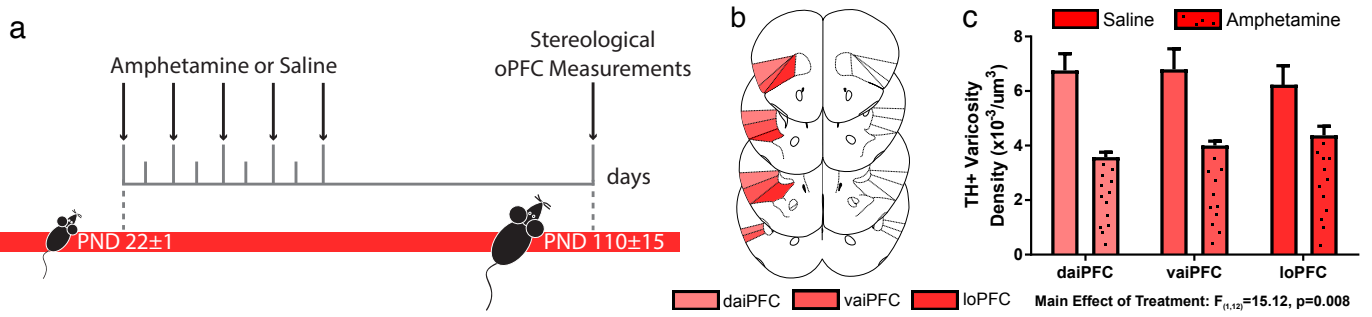
657

658 **Figure 4-2.** Dopamine (tyrosine hydroxylase immunopositive) varicosity density estimates  
659 for the piriform cortex in adult mice treated with either saline or amphetamine in early

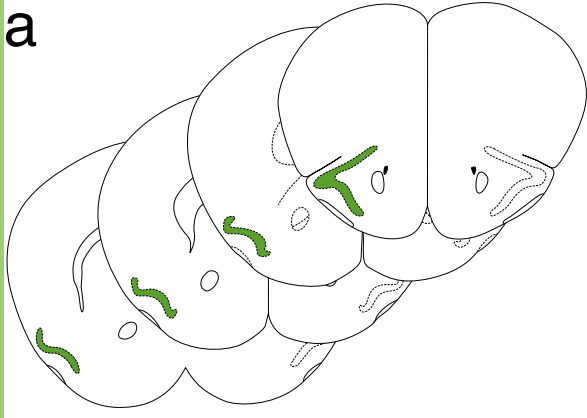
660 adolescence. Varicosity density was estimated by combining the optical fractionator and  
661 Cavalieri estimator methods of the software program Stereoinvestigator (see Methods).  
662 This data was used to generate the results presented in Results section 3.4 and Figure 4c.



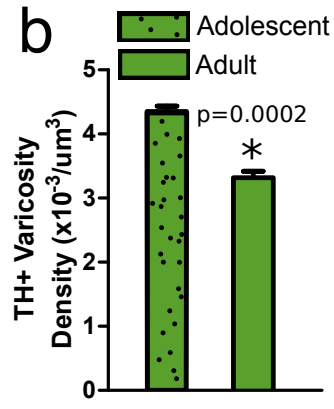




a



b



c

